

# INVESTIGATION OF CONVECTION AND RADIATION HEAT TRANSFER IN RHOMBUS MICROCHANNELS

C. Aghanajafi, V. Vandadi & M.R. Shahnazari

Department of Mechanical Engineering, K.N. Toosi University of Technology, Tehran, Iran

## ABSTRACT

The extensive engineering applications of Micro-Electro-Mechanical systems (MEMS) have promoted abundant studies of its fluid flow and heat transfer characteristics. This work presented numerical simulation of fully developed flow for characteristic laminar slip flow and heat transfer in rhombus microchannels with the presence of radiation. The slip velocity and temperature jump boundary conditions at the wall are performed. The effects of Reynolds number, velocity slip and temperature jump on Poiseuille number and impact of the presence of radiation on Nusselt number for different aspect ratio is reported.

**Keywords:** MEMS, Microchannel, Radiation, Rhombus, Slip Flow, Velocity slip, Temperature jump

## 1. INTRODUCTION

Analysis of fluid transport at microscale is of a great importance not only for playing a key role in the biological systems, but also in a wide variety of contemporary engineering applications, involving micro-scale devices such as microsensors, micropumps, and cooling electronic equipments. Microchannels however are the basic structure of these systems. People realize that there are many differences between heat and flow transfer in Microchannels and channels with conventional size.

A number of practical situations involve heat transfer between a low-density gas and a solid surface. In employing the term low density, we shall mean those circumstances where the mean free path of the gas molecules is no longer small in comparison with a characteristic dimension of the heat transfer surface. The mean free path is the distance a molecule travels, on the average, between collisions. The larger this distance becomes, the greater the distance required to communicate the temperature of a hot surface to a gas in contact with it. Evidently, the parameter which is of principal interest is a ratio of the mean free path to a characteristic body dimension. This grouping is called the Knudson number which is defined as:

$$Kn = \frac{\lambda}{L} \quad (1)$$

Beskok and Karniadakis [1] classified the gas flow in microchannels into four flow regimes. They are continuum flow regime ( $Kn \leq 0.001$ ), slip flow regime ( $0.001 < Kn \leq 0.1$ ), transition flow regime ( $0.1 < Kn \leq 10$ ) and free molecular flow regime ( $Kn > 10$ ).

In slip flow regime, the Navier-Stokes and energy equations remain applicable, provided a velocity slip and temperature jump are taken into account at the walls. Researchers have investigated theoretical, numerical and experimental studies in microchannels along with velocity slip and temperature jump boundary condition at the walls [2-8]. Numerical analysis of fully developed laminar slip flow and heat transfer in trapezoidal microchannels had been studied by Bin et al. [3] with uniform wall heat flux boundary condition. In their investigation, the influence of velocity slip and temperature jump on friction factor and Nusselt number were investigated in detail. M. Shams and C. Aghanajafi has studied numerical simulation of slip flow through rhombus microchannels without the impact of heat transfer through radiation [9]. Wei et al. [10] investigated the steady state convective heat transfer for laminar, two dimensional, incompressible rarefied gas flow by the finite volume finite difference scheme with slip flow and temperature jump boundary conditions.

In this paper, a fully developed laminar flow in a rhombus microchannel with the presence of radiation is investigated. Numerical results are obtained using a continuum based three dimensional, incompressible, steady model which is solved by a finite-volume method with slip velocity and temperature jump boundary conditions applied to the momentum and energy equations, respectively. The effects of rarefaction and aspect ratio on Poiseuille number and Nusselt number are studied. The influence of the presence of radiation on Nusselt number is obtained.

## 2. NOMENCLATURE:

AR	Aspect ratio
L	Characteristic length
V	Magnitude velocity of fluid
U	Mean velocity
P	Pressure
x, y	Cartesian coordinates
T	Temperature
t	Tangential direction
n	Normal direction
H	Perpendicular diameter of channel
b	Horizontal diameter of channel
S	Cross-section area
k	Thermal conductivity
h	Heat transfer coefficient
u	Streamwise velocity
v	Normal velocity
w	Bi-normal velocity
q <sub>r</sub>	Heat transfer through radiation
Kn	Knudsen number
Pr	Prandtl number
Po	Poiseuille number
Re	Reynolds number
Nu	Nusselt number
c <sub>p</sub>	Specific heat at constant pressure
U <sub>inlet</sub>	Inlet velocity
T <sub>inlet</sub>	Inlet temperature
D <sub>h</sub>	Hydraulic diameter of channel
<i>Greek symbols</i>	
λ	Mean free path
ρ	Density of fluid
μ	Dynamic viscosity of fluid
γ	Specific heat ratio of fluid
τ	Second order stress tensor
Φ	Ratio of Poiseuille number at Kn=0 to Poiseuille number at non-zero Kn
σ <sub>v</sub>	Tangential momentum accommodation coefficient
σ <sub>T</sub>	Thermal accommodation coefficient

## 3. MODEL SETUP

In this paper, microchannels with rhombus cross section are analyzed. The simulations are performed based on the following assumptions:

- (1) The governing equations based on Navier-Stokes equations associated with slip boundary conditions that can describe slip flow regimes in microchannels.
- (2) The flow is laminar.
- (3) The process is three-dimensional incompressible steady flow.
- (4) The body forces are neglected.
- (5) The energy equation with the presence of radiation is applied.

The resulting governing equations are following:

Continuity equation:

$$\frac{\partial u_k}{\partial x_k} = 0 \quad (2)$$

Momentum equation:

$$\rho \frac{\partial (u_k u_j)}{\partial x_k} = -\frac{\partial p}{\partial x_j} + \mu \left( \frac{\partial u_j}{\partial x_k} + \frac{\partial u_k}{\partial x_j} \right) \quad (3)$$

where,  $u$  is the velocity component,  $p$  is pressure,  $\rho$  is the fluid density,  $\mu$  is the dynamic viscosity.

Energy equation:

$$\rho c_p \left( u_i \frac{\partial T}{\partial x_i} \right) = k \frac{\partial^2 T}{\partial x_i \partial x_i} - \frac{\partial q_r}{\partial x_i} \quad (4)$$

where,  $T$  is temperature, and  $c_p$  is the specific heat at constant pressure.

$$q_r(x_i) = \frac{-4\sigma}{3k} \frac{\partial T^4}{\partial x_i} \quad (5)$$

where  $\sigma$  is the Stefan-Boltzman constant and  $k$  is the Rosseland mean absorption coefficient. Assuming that the optical depth of the gas is sufficiently large and the temperature gradients are sufficiently small so that the local intensity results from local emissions and also  $T^4$  can be expressed as a linear function of temperature

$$T^4 \cong 4T_\infty^3 T - 3T_\infty^4 \quad (6)$$

where the higher order terms of the expansion are neglected.

The most common means of analytically or numerically modeling a rarified flow within the slip flow regime,  $0.01 \leq Kn \leq 0.1$ , is through the use of slip velocity and temperature jump boundary conditions applied to the conventional continuum momentum and energy equations. The original slip velocity boundary condition and temperature jump boundary condition were derived by Maxwell [11] and Smoluchowski [12], respectively.

$$u_{fluid} - u_{wall} = \left[ \left( \frac{2-\sigma_v}{\sigma_v} \lambda \right) \left( \frac{\partial u}{\partial y} \right)_{wall} + \left( \frac{3\mu}{4\rho T} \right) \left( \frac{\partial T}{\partial x} \right)_{wall} \right] \quad (7)$$

$$T_{fluid} - T_{wall} = \left[ \left( \frac{2-\sigma_T}{\sigma_T} \frac{\gamma}{\gamma+1} \frac{\lambda}{Pr} \right) \left( \frac{\partial T}{\partial y} \right)_{wall} \right] \quad (8)$$

where,  $u$  is the tangential velocity,  $\lambda$  is the mean-free path of the molecules,  $\sigma_v$  is the tangential momentum accommodation coefficient,  $\sigma_T$  is the thermal accommodation coefficient,  $\gamma$  is the specific heat ratio of the gas,  $Pr$  is the Prandtl number,  $\mu$  is the viscosity,  $\rho$  is the density and  $T$  is the temperature of the gas at the wall.

The first term in eq.(7) is the velocity slip due to the shear stress at the solid surface, and the second term is the thermal creep velocity due to a temperature gradient tangential to the wall. These equations are presented in a format assuming a Cartesian coordinate system, a wall normal direction ( $y$ ), and a streamwise direction ( $x$ ).

It should be noted that the streamwise velocity and the temperature at the inlet are uniform and other component of velocity are zero. The wall temperature is constant. The velocity gradients along the axial flow direction are zero which means the boundary condition at the outlet boundary is outflow. Obviously, the channel length is chosen so that the developing length can be neglected in comparison with the developed flow length and there is thermally and hydrodynamically developed flow at the outlet boundary.

The tangential momentum accommodation and the thermal accommodation coefficients vary between zero and unity. The tangential momentum accommodation coefficient is zero for specular molecular reflection at the wall and it is unity for diffuse reflection [13]. The thermal accommodation coefficient is zero if molecules hold their original temperature upon collision and it is unity if they gain the wall temperature. In this paper these coefficients are assumed as unity. The specific heat ratio of the gas  $\gamma$  is equal to 1.4.

#### 4. NUMERICAL MODEL

In this paper the rhombus microchannel is studied. The aspect ratio  $AR$  is defined as:

$$AR = \frac{H}{b} \quad (9)$$

where,  $H$  and  $b$  are horizontal and vertical diameters of the rhombus channel, respectively. In order to reach fully developed condition the length is sufficiently long.

The 3D, incompressible, laminar, steady state momentum and energy equations are used. The commercial CFD software FLUENT<sup>TM</sup> [15] version 6.0.12 is employed to solve the governing equations. The SIMPLEC is used to link the pressure and velocities. In order to ensure the fineness of the computational grid spacing a grid

independency test is performed. To investigate the influences of the slip boundary conditions a code is included in FLUENT™ v.6.0.12. The residuals are considered  $10^{-6}$  to reach accurate results and convergence of the solution. A grid independency check is included to ensure that the solution is independent of grid size.

## 5. VALIDATION

To establish that the numerical procedure accurately models the slip flow regime, some comparisons are performed. Poiseuille numbers have been compared with analytical values according to  $Po=24/(1+12Kn)$  in Table 1 that shows good agreement. In Table 2, the Nusselt number have been compared with the results of Reinksizbulut [7] for  $Kn=0$  through a range of Reynolds number. The comparisons have been performed for parallel plates. The aspect ratio has been chosen sufficiently large that the channel geometry tends to parallel plates. Another case of validation is presented in Table 3 in which contains the results of this research and the results of Morini[14]. The results are completely in accord with the Morini's results for different value of  $\Phi$  ( $\Phi$  is the ratio of Poiseuille number at  $Kn=0$  to Poiseuille number at non-zero  $Kn$ ).

## 6. RESULTS AND DISCUSSION

### 6.1. Fully developed non-dimensional velocity

The non-dimensional maximum velocity and velocity slip for  $AR=1$  and varying Knudson number are shown in Figure 1. As shown in this figure the velocity at the wall is zero for  $Kn=0$ . This figure shows that the velocity slip at the wall increases with increasing  $Kn$ , which means that the slip velocity increases as the effect of rarefaction becomes more significant. Also it is obvious in this figure that the maximum velocity in the center of the channel decreases, when Knudson number increases. The variations of the fully developed non-dimensional maximum velocity and velocity slip with different aspect ratio and  $Kn=0.01$

Table 1 Fully developed Poiseuille number for parallel plates.

Knudsen number	Poiseuille number Analytical Results	Present Results	%
0	24	23.9741	0.11
0.005	22.64	22.6117	0.13
0.01	21.43	21.3524	0.36
0.05	15	15.064	0.43
0.1	10.91	10.9845	0.68

Table 2 Fully developed Nusselt number for parallel plates.

Reynolds number	Results of Reinksizbulut [7]	Present Results
0.1	8.105	8.124
1	8	8.046
5	7.741	7.801
10	7.624	7.660

Table 3 Fully developed Poiseuille number for rectangular microchannel.

	$Kn=0$		$Kn=0.001$		$Kn=0.01$		$Kn=0.1$	
	Results of [14]	Present results	Results of [14]	Present results	Results of [14]	Present results	Results of [14]	Present results
Aspect ratio	$\Phi$	$\Phi$	$\Phi$	$\Phi$	$\Phi$	$\Phi$	$\Phi$	$\Phi$
1	14.227	14.211	0.992	0.992	0.926	0.928	0.565	0.571
0.6	14.979	14.939	0.992	0.992	0.923	0.924	0.551	0.556
0.2	19.071	18.944	0.99	0.99	0.907	0.91	0.496	0.506

are shown in Figure 2. As shown in this figure, the maximum velocity in the center of the channel decreases when the aspect ratio of the channel increases. It is shown that, increasing the value of aspect ratio augments the slip velocity.

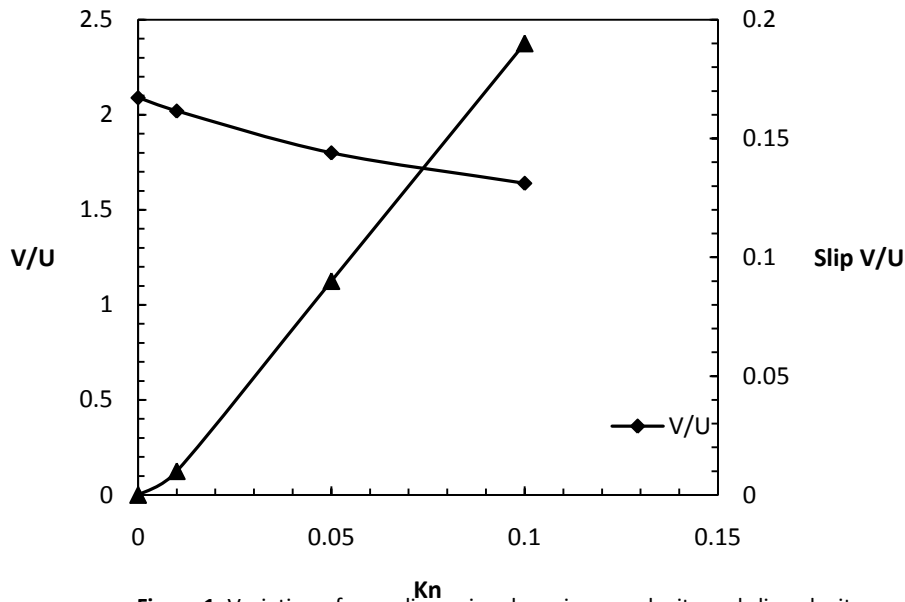


Figure 1. Variation of non-dimensional maximum velocity and slip velocity with Knudsen number

### 6.2. Hydrodynamic characteristics

Poiseuille number is one of the most important parameters in fluid flow which is the product of friction factor and local Reynolds number. The effects of rarefaction, aspect ratio and Reynolds number on Poiseuille number on rhombus microchannels are shown below. Figure 3 shows the influence of Reynolds number on Poiseuille number for different rarefactions and unity aspect ratio.

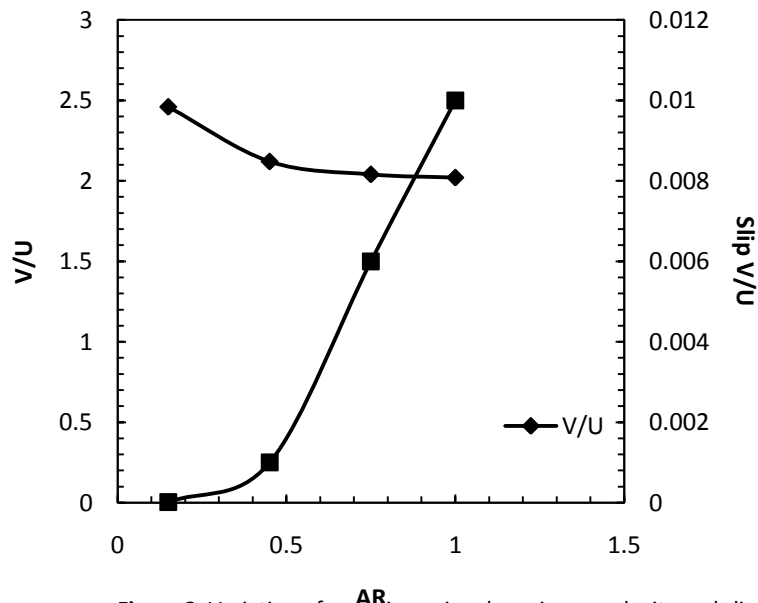


Figure 2. Variation of non-dimensional maximum velocity and slip velocity with aspect ratio

As seen in Figure 3, the variations of Reynolds number have little effect on Poiseuille number for a fixed rarefaction. It can be concluded from this figure that Poiseuille number decreases with increasing value of Knudson number. Figure 4 shows the Poiseuille number as a function of aspect ratio for different Reynolds number and at  $Kn=0.01$ . As seen in Figure 4, Poiseuille number increases with increasing value of aspect ratio, and as shown in this figure, the variations of Reynolds number have little influences on Poiseuille number. Variation of fully developed Poiseuille number with aspect ratio for different Knudsen number at  $Re=10$  is the purpose of Figure 5. It is obvious in Figure 5 that Poiseuille increases with increasing value of aspect ratio for a fixed Knudsen number. As seen in this figure the aspect ratio is more effective when it is less than 0.7 and at greater values than this aspect ratio, the Poiseuille number is constant for a fixed rarefaction. This figure also shows that Knudsen number can considerably affect on Poiseuille number, in which Poiseuille number reaches its maximum when Knudsen number is equal to zero, i.e. no slip condition, and then increasing the value of rarefaction reduces the value of Poiseuille number.

### 6.3. Heat transfer

The most important parameter in heat transfer is the ratio of convective to conductive heat transfer across the boundary which is called Nusselt number. The average local heat transfer or the local Nusselt number is defined as:

$$Nu = \frac{hD_h}{k} = \frac{D_h \left( \left( \frac{\partial T}{\partial x} \right)_{wall} \right)_x}{T_{wall} - T_m} \quad (10)$$

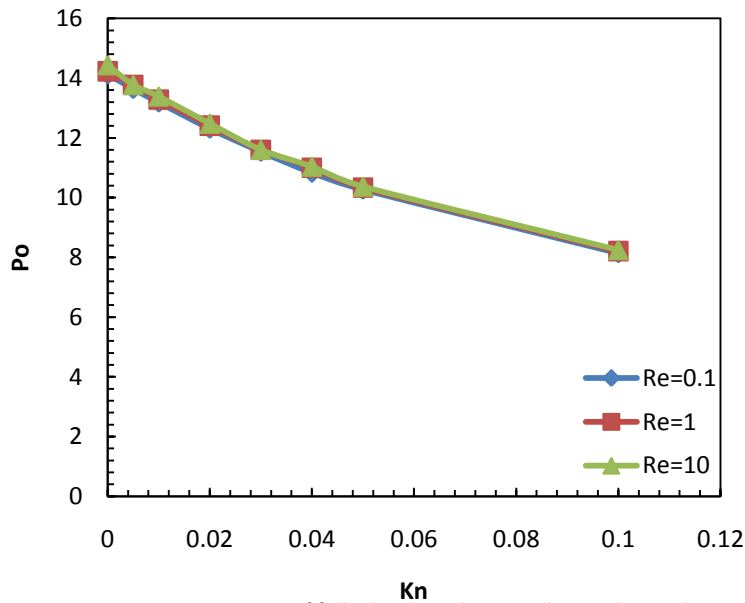


**Figure 3.** Variation of fully developed Poiseuille number with Knudson number for different Reynolds number at aspect ratio=1

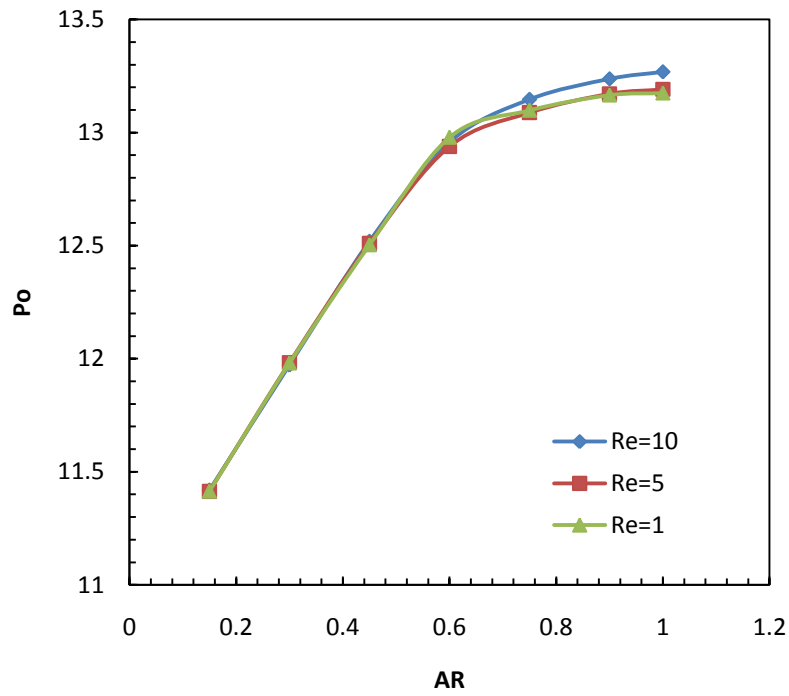


**Figure 4.** Variation of fully developed poiseuille number with aspect ratio with different reynolds number at Kn=0.01

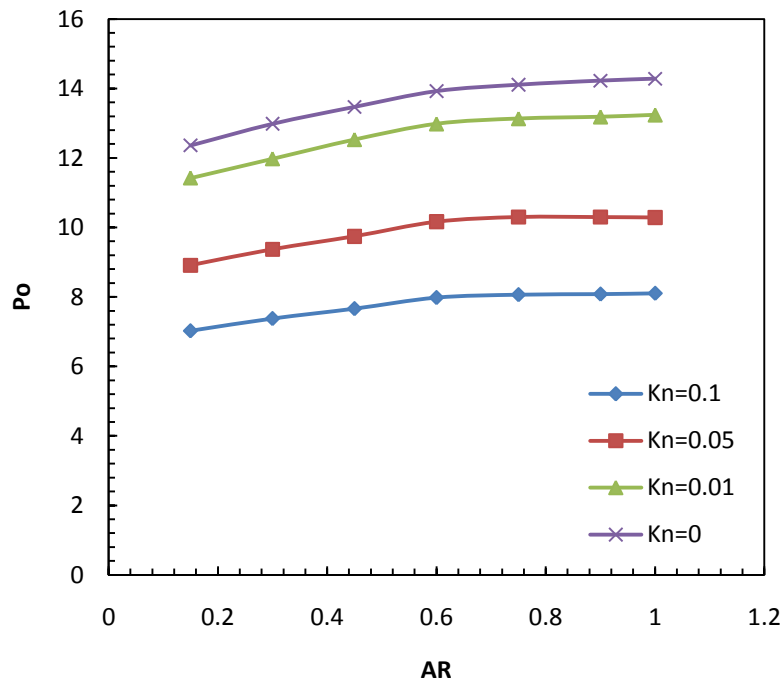


**Figure 5.** Variation of fully developed poiseuille number as a function of Knudson number and aspect ratio for Re=10

where,  $h$  is the heat transfer coefficient,  $\left(\frac{\partial T}{\partial x}\right)_{wall}$  is the circumferentially average temperature gradient to the wall and  $T_m$  is the bulk mean temperature.

In order to study the influence of the presence of Radiation the heat transfer coefficient is defined as:

$$h = h_{conv} + h_{rad} \tag{11}$$

where,  $h_{conv}$  is the convective heat transfer coefficient and  $h_{rad}$  is the heat transfer coefficient of radiation. Obviously, when the radiation is neglected, the total heat transfer coefficient is equal to convective heat transfer coefficient.

The figures following are the results of investigations which show the effects of Reynolds number, Prandtl number, Knudsen number and channel aspect ratio on fully developed Nusselt number for microchannel with rhombus cross section. The effect of the presence of radiation on Nusselt number is shown and discussed in details. Figure 6 shows the effect of Prandtl number on Nusselt number for different aspect ratio at  $Re=10$  and  $Kn=0.01$ . It is obvious that increasing the value of Prandtl number causes the reduction in temperature jump and consequently reduces the heat transfer rate and the Nusselt number. It is shown in this figure that the Nusselt number increases by increasing the value of aspect ratio of the channel. Also it can be seen in this figure that the presence of the radiation augments the value of Nusselt number. Figure 7 shows the Nusselt numbers as a function of aspect ratio for different Reynolds

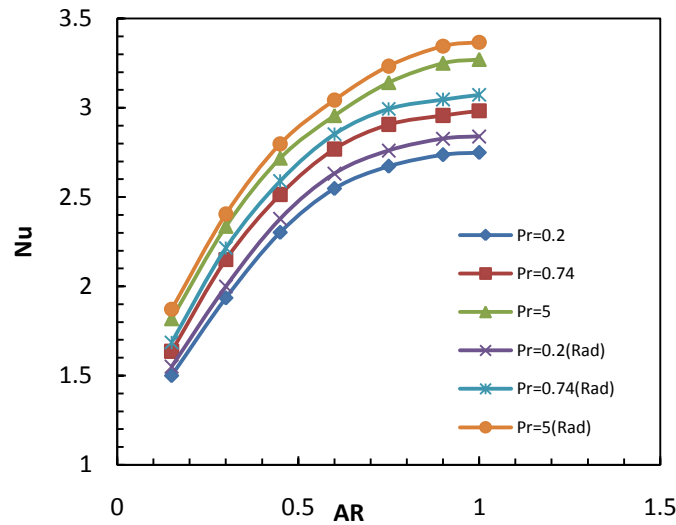


Figure 6. Effect of Prandtl number on Nusselt number for different aspect ratio for  $Re=10$

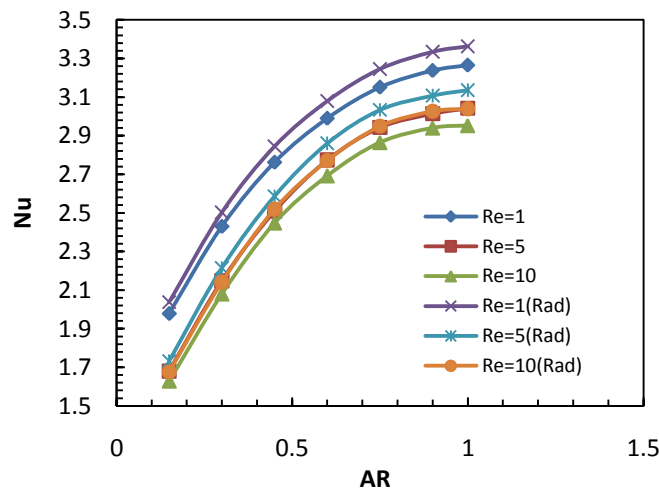
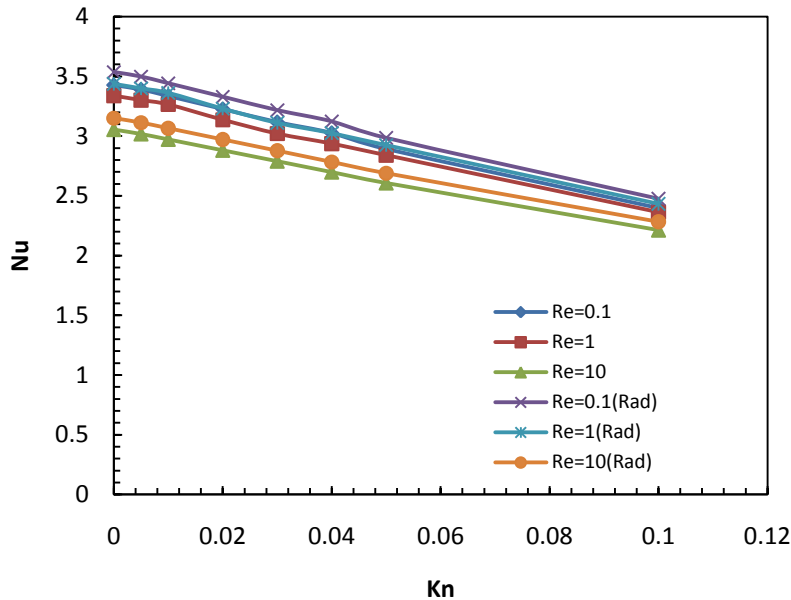
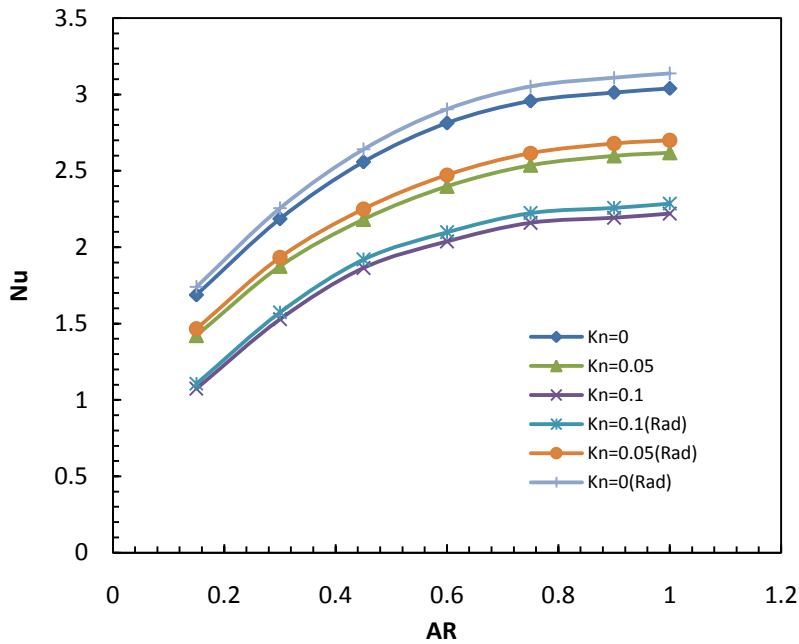


Figure 7. Variation of Nusselt number with aspect Ratio for different Reynolds number at  $Pr=0.74$  and  $Kn=0.01$

numbers for  $Kn=0.01$  and  $Pr=0.74$ . It is clear in this figure that the heat transfer rate decreases with increasing the value of Reynolds number and this reduction is greater between lower value of Reynolds number. Also it is shown that the Nusselt number increases when the aspect ratio of the channel increases for a fixed Reynolds number. The influence of the presence and absence of radiative heat transfer is also depicted in this figure. Figure 8 shows the Nusselt number as a function of rarefaction for different Reynolds number at  $Pr=0.74$  and aspect ratio of unity. The effect of radiation is clearly shown in this



**Figure 8.** Variation of Nusselt number with Knudson number for different Reynolds number at  $Pr=0.74$  and aspect Ratio=1



**Figure 9.** Variation of fully developed Nusselt number as a function of Knudson number and aspect ratio at  $Re=10$ ,  $Pr=0.74$

figure. It is shown in this figure that the value of Nusselt number is greater for lower Reynolds number, and also the Nusselt number decreases with increasing the value of rarefaction. The variation of fully developed Nusselt number as a function of aspect ratio and Knudsen number is investigated and shown in Figure 9 at  $Re=10$  and  $Pr=0.74$ . As seen in Figure 9, the Nusselt number has its maximum value when there are no rarefaction and it is obvious in this figure that the rarefaction causes reduction in heat transfer rate and Nusselt number for a fixed aspect ratio. It is clearly shown in this figure that decreasing the value of aspect ratio for a fixed Knudsen number affects the Nusselt number in which it reduces and lower aspect ratios have more considerable effects on this reduction. We can also see in this figure that the presence of radiation has a magnificent effect on the heat transfer rate i.e. Nusselt number.

## 7. CONCLUSION

A three dimensional incompressible steady model has been developed to investigate the effects of Reynolds number, aspect ratio, rarefaction, Prandtl number and radiation heat transfer on Poiseuille and Nusselt number for fully developed laminar flow over a range of slip flow regime in a microchannel with rhombus cross section. Constant wall temperature, slip velocity and temperature jump boundary conditions were included. The Nusselt and Poiseuille number both decrease with decreasing the value of aspect ratio, but rarefaction has inverse effect on Poiseuille and Nusselt number in which Poiseuille and Nusselt number decreases with increasing in Kn. It is observed from the figures that Reynolds number has more effect on Nusselt number then Poiseuille number. It is concluded from the figures and results that the presence of the radiation augments the heat transfer rate and Nusselt number to about 3% in comparison by the absence of radiation.

## 8. REFERENCES

- [1] A. Beskok, G.E. Karniadakis, Simulation of heat and momentum transfer in complex micri-geometries, *Journal of Thermo Physics and Heat Transfer* 8(1994) 647-653
- [2] C.B. Sobhan, S.V. Garmilla, A comparative analysis of studies on heat transfer and fluid flow in microchannels, *Microscale Thermophysical Engineering* 5 (2001) 293-311
- [3] Bin C, Guang WC, Quan Y. Fully developed laminar flow and heat transfer in smooth trapezoidal microchannel. *International Communication in Heat and Mass Transfer* 2005;32:1211-20
- [4] Orhan A, Mete A. Heat and fluid flow characteristics of gases in micropipes. *International Journal of Heat and Mass Transfer* 2006;49:1723-30
- [5] Mohamed GH. The fluid mechanics of microdevices. *Journal of Fluid Engineering* 1999;121:5-33
- [6] J.Lui, Y.C, Tai, C.M. Ho, MEMS for pressure distribution studies of gaseous flows in microchannels, *Proceeding of IEEE International conference on Micro Electro Mechanical Systems, Amesterdam, Netherlands, 1995, pp. 209-215.*
- [7] M.Renksizbulut, H. Niazmand, G Tercan, Slip-flow and heat transfer in rectangular microchannels with constant wall temperature, *International Journal Thermal Sciences* 45 (2005) 870-881.
- [8] T.T. Zhang, L. Jia, Z.C. Wang, C.W. Li, Slip Flow characteristics of compressible gaseous in microchannels, *Energy Conversion Management* 50 (2009) 1676-1681
- [9] M. Sahms, M. Shojaeian, C. Aghanajafi, A.R. Dibaji, Numerical simulation of slip flow through rhombus microchannels, *International Communication in heat and mass transfer, (2009) uncorrected proof*
- [10] Wei S, Sadik K, Yazicioglu Almila G, A numerical study of single phase convective heat transfer in microtubes for slip flow, *International Journal of Thermal Science* 2007;46:1084-94
- [11] J.C. Maxwell, On stress in rarified gases arising from inequalities of temperature, *Philosophical Transaction of the Royal Society of London* 170 (1879) 231-256
- [12] M. Smoluchowski, Ueber Wärmeleitung in Verdünnten Gasen, *Annalen der Physik und Chemie* 64 (1898) 101-130
- [13] A. Beskok, G.E. Karniadakis, Simulation of heat and momentum transfer in complex micro-geometries, *Journal of Thermo Physics and Heat Transfer* 8 (1994) 647-653
- [14] G.L. Morini, M. Spiga, P. Tartarini, The rarefaction effect on the friction factor of gas flow in microchannels, *Superlattices and Microstructures* 35 (2004) 587-599
- [15] Fluent, Inc, Fluent 6.0.12 User's Guide. Fluent. Inc., Centerra Resource Park, 10 Cavendish Court, Lebanon, NH 03766, 2001